RAA 2019 Vol. **19** No. **5**, 71(10pp) doi: 10.1088/1674–4527/19/5/71

http://www.raa-journal.org *http://iopscience.iop.org/raa*

***R**esearch in*
***A**stronomy and*
***A**strophysics*

CCD astrometric observations of 2017 VR12, Camillo and Midas

Zhen-Jun Zhang[1,2,3], Yi-Gong Zhang[1,2,3], Xiang-Ming Chen[1,2], Jian-Cheng Wang[1,2] and Jie Su[1,2]

[1] Yunnan Observatories, Chinese Academy of Sciences, Kunming 650216, China; *zjzhang@ynao.ac.cn*
[2] Key Laboratory of the Structure and Evolution of Celestial Objects, Chinese Academy of Sciences, Kunming 650216, China
[3] University of Chinese Academy of Sciences, Beijing 100049, China

Received 2018 June 21; accepted 2018 November 13

Abstract We have observed three near-Earth objects (NEOs), 2017 VR12, Camillo and Midas, during 2018. The observations were made with the 1-m telescope, operated by Yunnan Observatories, over two nights. Their precise astrometric positions are derived from 989 CCD observations. The theoretical positions of asteroids are retrieved from the Jet Propulsion Laboratory (JPL) Horizons System and Institut de Mécanique Céleste et de Calcul des Éphémérides (IMCCE). The positions of three asteroids are measured with respect to stars in the *Gaia* DR2 star catalog. For 2017 VR12, the means $(O-C)$ of right ascension and declination are $-0.090''$ and $-0.623''$ respectively based on the published JPL ephemeris, but the corresponding means $(O-C)$ are $3.122''$ and $-0.636''$ based on the published IMCCE ephemeris. The great difference in declination could be explained by several factors. (1) The degraded CCD images caused by the fast apparent motion of the objects lead to a reduction in positioning accuracy. (2) The poor timing system may introduce systematic errors, especially in the high speed direction. (3) The asteroid may be perturbed by Earth when it approaches the Earth too closely. These astrometric results demonstrate that the centroid centering method can reduce the dispersion of non-Gaussian images as compared with the PSF modeling method. For Camillo and Midas, the astrometric results are consistent based on the two ephemerides. Implementing a high-precision timing system, and analyzing some astronomical effects and geometric distortions in CCD images should be carefully considered in future works.

Key words: astrometry: astrometric observation — NEOs: individual (2017 VR12, Camillo, Midas)

1 INTRODUCTION

Near-Earth object (NEO) research plays an increasingly important role not only in solar system science but also in protecting our planetary environment and human society from the hazards posed by asteroids and comets (Ticha et al. 2009). Near-Earth asteroids (NEAs) are asteroids with a perihelion distance of less than 1.3 AU. Potentially hazardous asteroids (PHAs) are NEAs that have minimum orbit intersection distances with the Earth of less than 0.05 AU and have an absolute magnitude $H < 22.0$ mag (Gronchi 2005; Perna et al. 2013). Continuous optical and radar observations are needed for accurate orbit determination and physical characterization, and special attention to their orbit monitoring is required (Nedelcu et al. 2010; Bancelin et al. 2012). Compared with all other asteroid populations, the NEA population has shorter periods, making it a reliable set of dynamical reference frame representatives. Optical data together with radar data can be used for constraining NEA dynamics and possibly revealing more subtle, non-gravitational effects such as the Yarkovsky effect (Nedelcu et al. 2010). Several national and international observational efforts have been devoted to detecting undiscovered NEOs and especially PHAs, to determine their orbital properties and impact probabilities, and to investigate their physical nature (Perna et al. 2013). Astrometric follow-up is also essential for targets of future radar observations, space missions and other observing campaigns. The *Gaia* Follow Up Network for Solar System Objects (*Gaia*-Fun-SSO) was established to coordinate astrometric follow-up observations (Thuillot et al. 2011). Many accurate astrometric observations are very

Table 1 Specifications of the 1-m Telescope and CCD Detector

Approximate focal length	1330 cm
F-ratio	13
Diameter of primary mirror	100 cm
CCD field of view	$7.1' \times 7.1'$
Size of CCD array	2048×2048
Size of pixel	$13.5\mu m \times 13.5\mu m$
Approximate angular extent per pixel	$0.21''$

useful for various purposes. In order to obtain accurate observations, some fundamental strategies are very important and should be implemented. For NEOs, due to their high velocity, we require a quick readout but also a CCD camera with good time recording capability to obtain high quality images. For all of the astrometric observations, we used the 2×2 pixel binning mode to reduce the readout time and readout noise. We estimated the accuracy of time recording and its effect on the astrometry results of NEAs. A reference star catalog is key to deriving the precise and accurate positions of NEAs, so we chose the newest and most precise star catalog, *Gaia* Data Release 2 (DR2) (Gaia Collaboration et al. 2016, 2018), as our reference star catalog. We have observed three NEAs, 2017 VR12, (1981) Midas and (3752) Camillo, using the 1-m telescope, operated by Yunnan Observatories, in March 2018. In Section 2, details of the observations are described. In Section 3, we present the methods used to measure the positions of three NEOs and estimate some important errors. In Section 4, we show the astrometric results and provide some discussion. We also make some comparisons with historical observations. Finally, we draw some conclusions in Section 5.

2 OBSERVATIONS

All the observations were acquired by the 1-m telescope administered by Yunnan Observatories with a 1.33 m equivalent focal length. More details about the telescope and CCD detector are listed in Table 1. The site (i.e. IAU code 286) is located at longitude E202.788° and latitude N25.0294°. All of the observations were made by using the 2×2 pixel binning mode.

The NEAs 2017 VR12 and Midas were identified as PHAs. 2017 VR12 is a sub-kilometer asteroid with a somewhat elongated and angular shape, and a diameter of about 160 m This V-type asteroid has a rotation period of approximately 1.5 hours. More details are provided in Table 2.

Information about observations of the three NEAs is given in Table 3. On the first night, all the observations were made with C filter. On the second night, some of the observations were made with I filter. For each of these asteroids, the total numbers of observations were 240 for 2017 VR12, 547 for Camillo and 202 for Midas. Flatfield and bias images were taken at the beginning of the observation. To reduce the readout noise and readout time, all of the observations were conducted using the 2×2 pixel binning mode.

3 ASTROMETRIC REDUCTION AND ERROR ESTIMATION

During the two day observing period, seeing at Yunnan Observatories was about $1.5'' \sim 2.5''$. All of the images targeting the three asteroids were corrected by bias and flatfield images, then the positions were measured with the software Astrometrica (`http://www.astrometrica.at/`). By applying the astrometric data reduction procedure, point spread function (PSF) fitting model method and centroid method, the center positions for the asteroids and reference stars were determined. To improve matching and processing speed, we selected stars brighter than 18 magnitude from the *Gaia* DR2 catalog as our reference stars. The reference stars are from the newest *Gaia* DR2 star catalog (Lindegren et al. 2018) which contains data on 1.7 billion star positions, and the median uncertainty in parallax and position at the reference epoch J2015.5 is about 0.04 mas for bright ($G < 14$ mag) sources, 0.1 mas at $G = 17$ mag and 0.7 mas at $G = 20$ mag. For descriptions of the measurement processes, please refer to Qiao et al. (2011, 2008).

For a CCD with a small field, we usually require no more than a linear fit. Using higher order fits always decreases the residuals for reference stars, unless the variation of the quadratic and cubic terms from one image to the next is significantly smaller than the value of these coefficients. A linear solution is probably an accurate representation of the true plate constants compared to a high order fit. Furthermore, it is noted that a reliable determination of higher orders in the plate constants is possible if there are many dozens of reference stars available for the solution (`http://www.astrometrica.at/`). In addition, when the number of reference stars available is just enough for the solution of high order plate constants due to the poor quality centering of some stars, an over-fitting situation may occur, causing a greater deviation from the true plate constants. Therefore, for the images with more than 12 reference stars, we choose the quadratic fit plate model

Table 2 Detailed Information about the Three Asteroids

Identification	Discoverer	Intersection distance (AU)	Magnitude	Motion velocity (arcsec min^{-1})		Apparent radius ($''$)	Phase ($^\circ$)
				d(RA)/dt×cosD	d(Dec)/dt		
2017 VR12	–	0.0077	≈12.5	2∼4	−23∼−42	0.006	53
3752 Camillo	E.F. Helin et al.	0.078	14.8	0.45	4.5	0.006	60
1981 Midas	C.T. Kowal	0.0034	14.3	−1.8	1.5	0.005	37

Table 3 Information about Observations of the Three NEAs

Target	Obs-Date	Exposure Time (s)	Filter*	No.
2017 VR12	20180304	8	C	144
	20180305	4	C	30
	20180305	4	I	66
3752 Camillo	20180304	6	C	272
	20180304	5	C	49
	20180305	8	C	179
	20180305	8	I	47
1981 Midas	20180304	6	C	96
	20180305	4	C	51
	20180305	20	C	19
	20180305	8	I	41
	20180305	20	I	22
	20180305	60	I	14

Notes: * Filter "C" stands for clean, a neutral color filter intended to keep the same optical path and "I" means infrared, which has effective wavelength midpoint $\lambda_{\rm eff} = 878$ nm.

to calibrate the CCD field, and for the rest, we choose the linear fit model.

Astronomical effects, such as the solar phase angle effect, are considered. In the case of phase correction, the phase angles and apparent radii are listed in Table 2. According to Lindegren (1977), a solar phase angle with light scattering on the surface of the asteroid causes an offset in its apparent positions, as described by Equation (1)

$$\begin{pmatrix} -\Delta\alpha\cos\delta \\ -\Delta\delta \end{pmatrix} = \begin{pmatrix} Cs\sin(i/2)\sin Q \\ Cs\sin(i/2)\cos Q \end{pmatrix}, \qquad (1)$$

where i is the solar phase angle, s is the apparent radius of the object, Q is the position angle of the sub-solar point in the tangential plane and C is a parameter related to the reflectance model adopted. For a spherical object, the value of C is about to 0.75.

The shapes of these three NEOs deviate significantly from a perfect sphere, so the exact phase correction cannot be obtained. However, we can estimate the phase corrections which are smaller than a few milliarcseconds. In view of the small CCD field of view, we choose the topocentric astrometric positions to compare the observational values with ephemeris ones. Considering the influence of atmospheric refraction and aberration, we should try to avoid the use of astrometric positions and replace them with the apparent positions to obtain more accurate astrometric positions in future work. We also estimate the errors associated with time recording. A CCD camera with good time recording capability is important for obtaining accurate observations. The time associated with the telescope control system is synchronized with GPS, but the time for controlling the CCD detector exposure is determined artificially. The unreliability of the timing system may introduces systematic error, especially for targets with fast apparent motion. We manually controlled the time error within 1 second during the observations. This error may cause large systematic errors for the high speed objects, especially 2017 VR12; more discussion will be given in Section 4. A fast-moving asteroid displays trails in its image (as seen in Fig. 1), and we adopted the PSF model and centroid centering method to compare the effects of non-Gaussian images on the astrometric result.

4 RESULTS AND DISCUSSION

We divided the observations into several groups to compare the effects of different exposures and filters on the

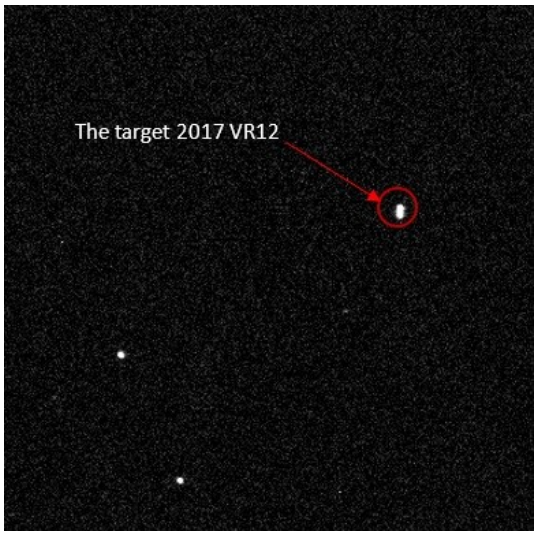

Fig. 1 Part of a typical CCD image of 2017 VR12 taken on 2018 March 5 at Yunnan Observatories with the 1-m telescope. The exposure time is 8 s.

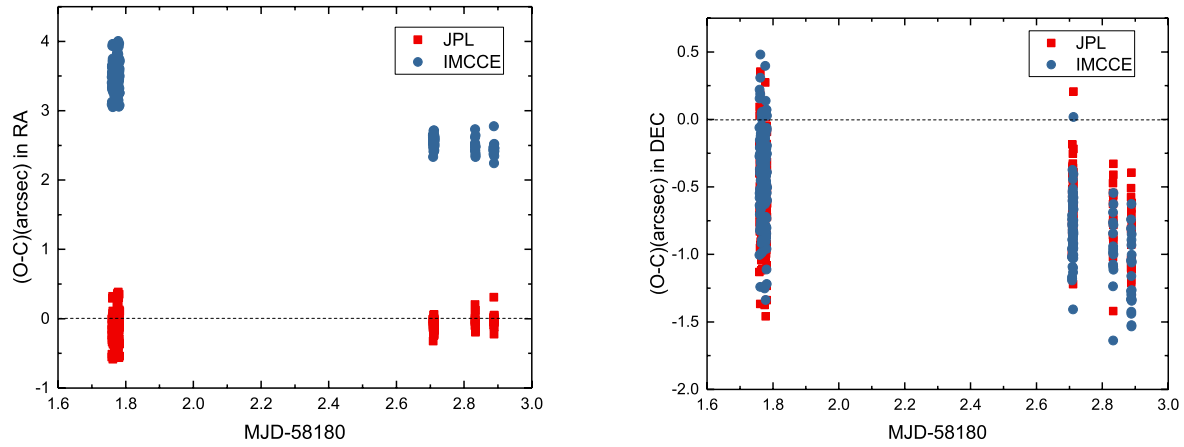

Fig. 2 The $(O-C)$ residuals of the position of 2017 VR12 using different ephemerides. The *red solid squares* represent the $(O-C)$ residuals using the DE431 ephemeris and the *blue solid circles* signify the $(O-C)$ residuals using the INPOP13c ephemeris. The target centering method adopts the PSF model method.

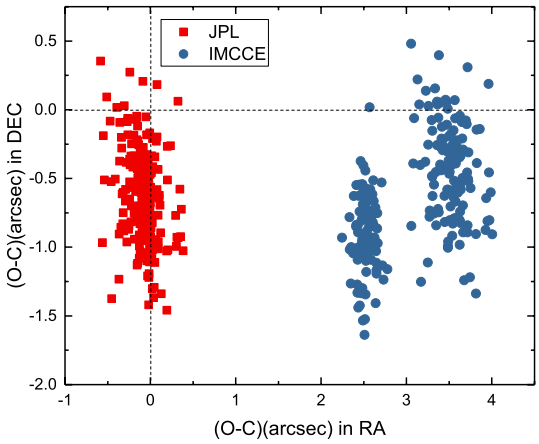

Fig. 3 The $(O-C)$ residuals of 2017 VR12 using different ephemerides. The *red points* represent the $(O-C)$ residuals using the DE431 ephemeris and the *blue ones* signify the $(O-C)$ residuals using the INPOP13c ephemeris. The target centering method adopts the PSF model method.

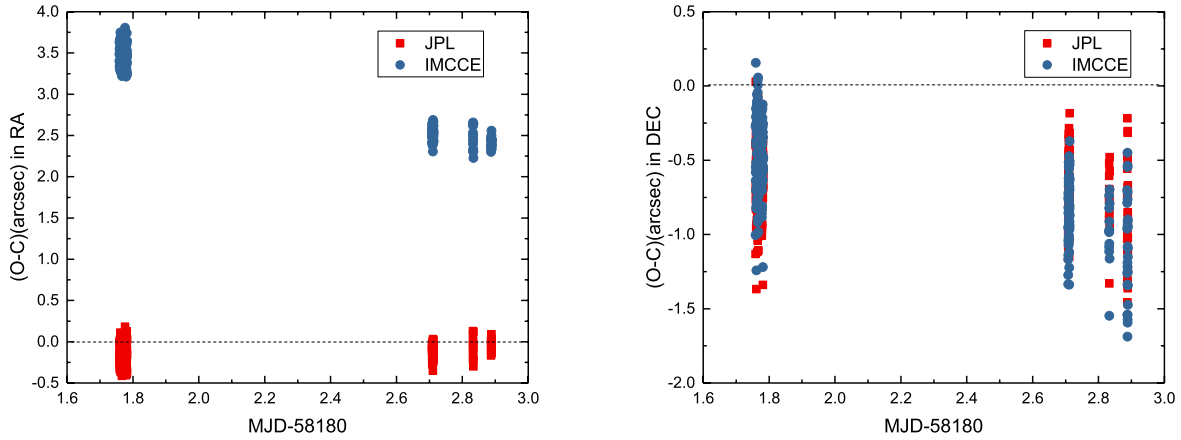

Fig. 4 The $(O-C)$ residuals of the position of 2017 VR12 using different ephemerides. The *red solid squares* represent the $(O-C)$ residuals using the DE431 ephemeris and the *blue solid circles* signify the $(O-C)$ residuals using the INPOP13c ephemeris. The target centering method adopts the centroid method.

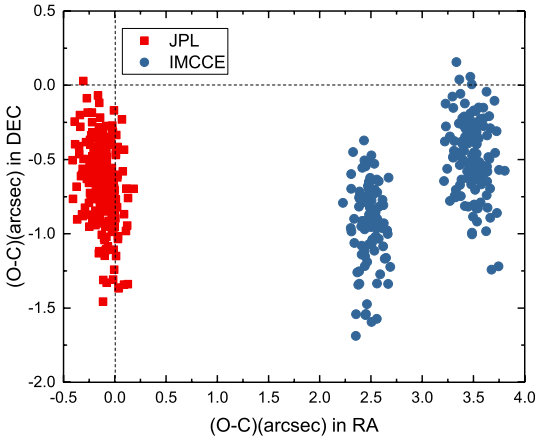

Fig. 5 The $(O-C)$ residuals of 2017 VR12 using different ephemerides. The *red points* represent the $(O-C)$ residuals using the DE431 ephemeris and the *blue ones* signify the $(O-C)$ residuals using the INPOP13c ephemeris. The target centering method adopts the centroid method.

astrometric results. We also compared the observed positions of three asteroids using the INPOP13c planetary ephemeris from Institut de Mécanique Céleste et de Calcul des Éphémérides (IMCCE, `http://www.imcce.fr/`) and DE431 from Jet Propulsion Laboratory (JPL, `http://ssd.jpl.nasa.gov/`).

4.1 2017 VR12

We give the statistics of astrometric results for 2017 VR12 in Tables 4 and 5 based on the PSF model and centroid method respectively. Column (1) lists information about the observations. For example, for '04-C8-1' and '05-I4-1', '04' indicates that the observation was made on 2018 March 4 and '05' means that the observation was made on 2018 March 5; 'C8' signifies that the filter is the C filter (i.e. clear filter) and the exposure time is 8 s; 'I4' means that the filter is the I filter; the last number of the first column indicates the observation sequence. The following columns list the mean $(O-C)$ and its standard deviation (SD) in right ascension and declination respectively. The 'JPL' and 'IMCCE' columns mean the asteroid ephemerides are from JPL (i.e. the DE431 planetary ephemeris) and IMCCE (i.e. the INPOP13c planetary ephemeris), respectively. All units are in arcsec and the reference stars are from the *Gaia* DR2 star catalog.

Figures 2 and 3 display the $(O-C)$ residuals of 2017 VR12 based on the PSF method. The mean values of $(O-C)$ in right ascension and declination are $-0.090''$ and $-0.623''$ based on the JPL ephemeris, and $3.122''$ and $-0.636''$ compared with the IMCCE ephemeris, respectively.

Figures 4–5 show the $(O-C)$ residuals of 2017 VR12 based on the centroid method. The mean values of $(O-C)$ in right ascension and declination are $-0.124''$ and

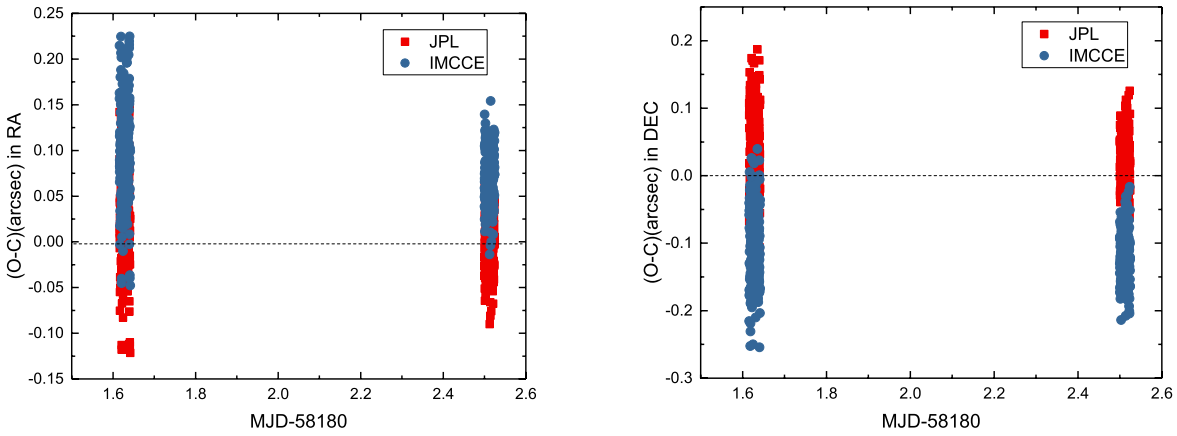

Fig. 6 The $(O-C)$ residuals of the position of Camillo using different ephemerides. The *red solid squares* represent the $(O-C)$ residuals using the DE431 ephemeris and the *blue solid circles* signify the $(O-C)$ residuals using the INPOP13c ephemeris.

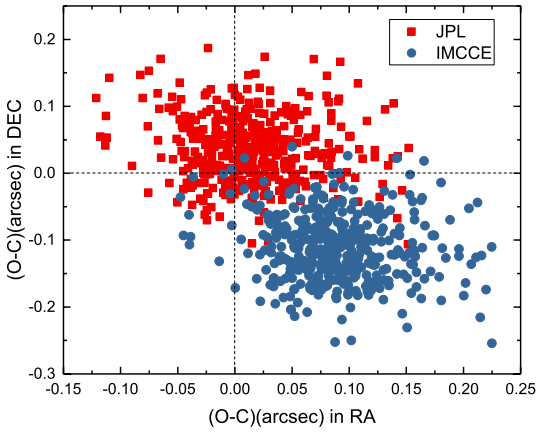

Fig. 7 The $(O-C)$ residuals of Camillo using different ephemerides. The *red points* represent the $(O-C)$ residuals using the DE431 ephemeris and the *blue ones* signify the $(O-C)$ residuals using the INPOP13c ephemeris.

Table 4 Statistics on $(O-C)$ Residuals for 2017 VR12, based on the PSF Model Method

	JPL				IMCCE			
2017 VR12	RA		Dec		RA		Dec	
	$\langle O-C\rangle$	SD	$\langle O-C\rangle$	SD	$\langle O-C\rangle$	SD	$\langle O-C\rangle$	SD
(1)	(2)	(3)	(4)	(5)	(6)	(7)	(8)	(9)
04-C8-1	–0.129	0.167	–0.542	0.343	3.507	0.167	–0.417	0.343
04-C8-2	–0.067	0.250	–0.570	0.411	3.554	0.250	–0.449	0.411
05-C4-1	–0.105	0.082	–0.645	0.216	2.551	0.082	–0.833	0.216
05-I4-1	–0.080	0.063	–0.637	0.219	2.575	0.063	–0.825	0.219
05-I4-2	–0.034	0.105	–0.718	0.270	2.493	0.105	–0.936	0.270
05-I4-3	–0.020	0.042	–0.927	0.271	2.447	0.042	–1.158	0.271
Total	–0.090	0.166	–0.623	0.330	3.122	0.547	–0.636	0.402

$-0.655''$ based on the JPL ephemeris, and $3.068''$ and $-0.659''$ compared with the IMCCE ephemeris, respectively. Our observations are more consistent with the ephemeris of JPL, especially in the right ascension direction.

The results of 2017 VR12 are inferior to those of Camillo and Midas. One of the reasons for this is the fast apparent motion. The images of 2017 VR12 were seriously distorted because of trailing, as depicted in Figure 1, especially in the declination direction. The distorted images lead to inaccuracy of centering, and thus the disper-

Table 5 Statistics on $(O-C)$ Residuals for 2017 VR12, based on the Centroid Method

	JPL				IMCCE			
2017 VR12	RA		Dec		RA		Dec	
	$\langle O-C\rangle$	SD	$\langle O-C\rangle$	SD	$\langle O-C\rangle$	SD	$\langle O-C\rangle$	SD
(1)	(2)	(3)	(4)	(5)	(6)	(7)	(8)	(9)
04-C8-1	−0.173	0.127	−0.574	0.157	3.463	0.126	−0.449	0.157
04-C8-2	−0.164	0.127	−0.598	0.181	3.457	0.127	−0.477	0.181
05-C4-1	−0.156	0.077	−0.673	0.219	2.501	0.077	−0.861	0.219
05-I4-1	−0.116	0.073	−0.638	0.223	2.539	0.073	−0.826	0.222
05-I4-2	−0.071	0.137	−0.772	0.222	2.455	0.137	−0.989	0.222
05-I4-3	−0.051	0.057	−0.856	0.347	2.416	0.057	−1.087	0.347
Total	−0.124	0.112	−0.655	0.273	3.068	0.536	−0.659	0.367

Table 6 Comparison with Other Observations

		JPL				IMCCE			
Site	No.	RA		Dec		RA		Dec.	
		$\langle O-C\rangle$	SD	$\langle O-C\rangle$	SD	$\langle O-C\rangle$	SD	$\langle O-C\rangle$	SD
(1)	(2)	(3)	(4)	(5)	(6)	(7)	(8)	(9)	(10)
K28	9	−0.657	0.212	2.280	0.610	1.865	0.216	2.053	0.610
Z80	18	−0.115	0.276	−0.396	0.245	3.232	0.279	−0.369	0.246
557	28	0.605	0.288	−0.073	0.172	8.149	0.455	1.366	0.195
L18	9	−0.316	0.284	0.190	0.143	4.290	0.283	0.637	0.143
This work	240	−0.090	0.166	−0.623	0.330	3.122	0.547	−0.636	0.402

Table 7 Statistics of $(O-C)$ Residuals for Camillo

	JPL				IMCCE			
Camillo	RA		Dec		RA		Dec	
	$\langle O-C\rangle$	SD	$\langle O-C\rangle$	SD	$\langle O-C\rangle$	SD	$\langle O-C\rangle$	SD
(1)	(2)	(3)	(4)	(5)	(6)	(7)	(8)	(9)
04-C6-1	0.028	0.051	0.044	0.058	0.101	0.051	–0.104	0.058
04-C6-2	0.033	0.075	0.046	0.060	0.106	0.075	–0.102	0.060
05-C5-1	–0.002	0.031	0.018	0.035	0.074	0.031	–0.126	0.035
05-C8-1	–0.007	0.029	0.025	0.042	0.069	0.029	–0.117	0.042
05-C8-2	0.009	0.032	0.020	0.035	0.085	0.032	–0.123	0.035
05-I8-1	0.005	0.035	0.043	0.048	0.081	0.035	–0.100	0.048
Total	0.014	0.048	0.035	0.051	0.088	0.047	–0.111	0.050

Table 8 Statistics of $(O-C)$ Residuals for Midas

	JPL				IMCCE			
Midas	RA		Dec		RA		Dec	
	$\langle O-C\rangle$	SD	$\langle O-C\rangle$	SD	$\langle O-C\rangle$	SD	$\langle O-C\rangle$	SD
(1)	(2)	(3)	(4)	(5)	(6)	(7)	(8)	(9)
04-C6-1	−0.006	0.119	−0.028	0.065	−0.217	0.119	−0.018	0.065
05-C4-1	−0.023	0.061	−0.087	0.046	−0.241	0.061	−0.080	0.046
05-C20-1	−0.059	0.053	−0.055	0.039	−0.277	0.053	−0.047	0.039
05-I8-1	−0.034	0.054	−0.042	0.039	−0.252	0.054	−0.035	0.039
05-I20-1	−0.032	0.043	−0.053	0.033	−0.250	0.043	−0.046	0.033
05-I60-1	−0.037	0.106	−0.048	0.062	−0.255	0.106	−0.041	0.062
Total	−0.023	0.081	−0.047	0.058	−0.239	0.080	−0.038	0.058

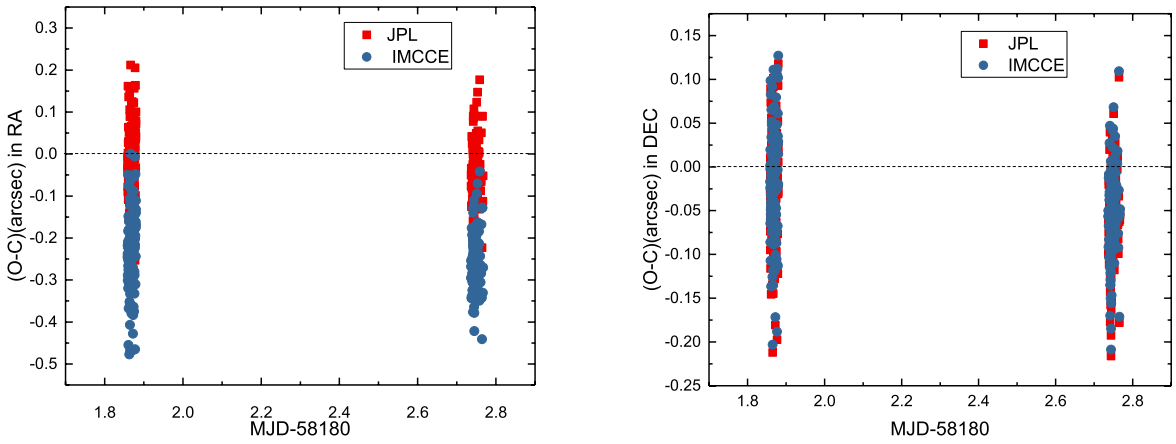

Fig. 8 The $(O-C)$ residuals of the position of Midas using different ephemerides. The *red solid squares* represent the $(O-C)$ residuals using the DE431 ephemeris and the *blue solid circles* signify the $(O-C)$ residuals using the INPOP13c ephemeris.

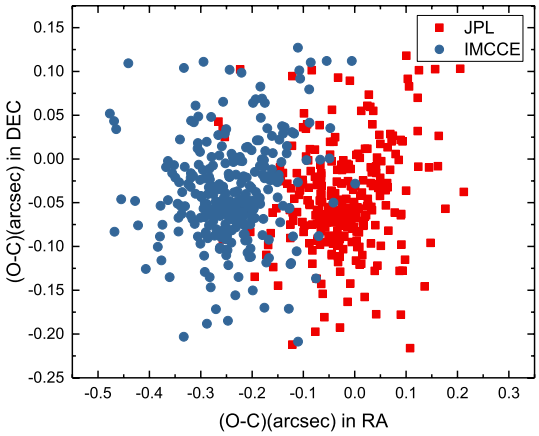

Fig. 9 The $(O-C)$ residuals of Midas using different ephemerides. The *red points* represent the $(O-C)$ residuals using the DE431 ephemeris and the *blue ones* signify the $(O-C)$ residuals using the INPOP13c ephemeris.

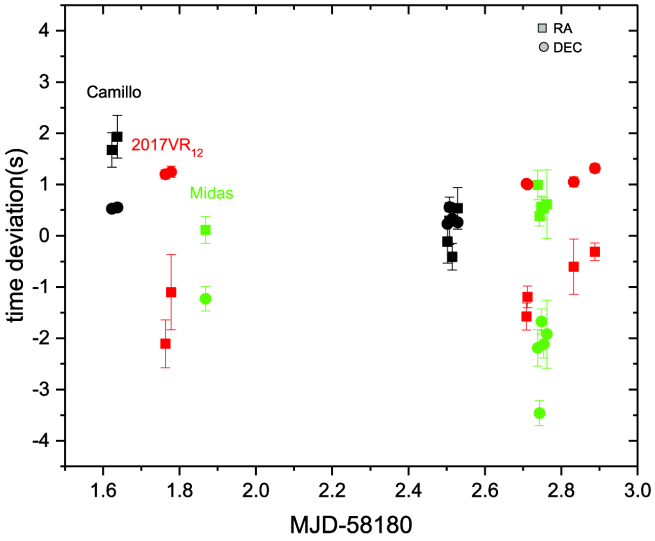

Fig. 10 TD estimation based on the astrometric results. The *squares* represent the TD based on astrometric results in right ascension and the *circles* signify TD based on astrometric results in declination. The *black points* come from Camillo, the *red ones* come from 2017 VR12 and the *green ones* come from Midas.

sion of $(O-C)$ residuals is larger. For positioning precision, 4 s of exposure time is better than 8 s. As seen in Table 2, the velocity component in the declination direction is larger than that in the right ascension direction, so the dispersion in the declination direction is larger. We adopted the PSF model and centroid methods to compare the effects of non-Gaussian images on the astrometric results. It can be seen that the astrometric results based on the centroid method have a smaller dispersion, especially when the exposure time is set as 8 s and the image degrades badly. However, the results based on the PSF model are in better agreement with the JPL ephemeris. The two centering methods show significant systematic differences. The timing system of image acquisition should be noted. The time of the telescope control system is synchronized with GPS, but the time to control the CCD detector exposure was determined artificially. The unreliability of the timing system may introduce systematic errors for mean $(O-C)$, especially for quickly moving objects. Finally, the asteroid may be perturbed by the Earth when it approaches Earth too closely, and the ephemeris might not be very accurate (Zhang et al. 2015). We can realize this from differences between the JPL and IMCCE ephemerides.

To compare our observations with others, we also list some historical observation results from other sites (`http://www.minorplanetcenter.net/`). Table 6 provides some typical residuals of the observations. It can be seen that all of the observations do not agree well with the ephemerides. The most likely reason is the lack of high-precision observational data, which limits the precision of ephemerides. The degraded image could be the main cause of the large dispersion in declination of our work.

4.2 Camillo

As shown in Figures 6 and 7 and Table 7, we compare the $(O-C)$ residuals of Camillo by using different ephemerides. The mean values of $(O-C)$ in right ascension and declination for Camillo are $-0.014''$ and $0.035''$ compared with the JPL ephemeris, and $0.088''$ and $-0.111''$ compared with the IMCCE ephemeris respectively. The dispersions of our observations are estimated to be about $0.048''$ and $0.051''$ in right ascension and declination respectively. We can see that the two ephemerides show good agreement, especially in right ascension. It seems that the DE431 ephemeris of JPL has better precision than the INPOP13c ephemeris in the right ascension direction. In addition, the results of Camillo are better than those of 2017 VR12, and one of the reasons for this is that images of Camillo have a sufficient number of reference stars. The number of reference stars in images of Camillo is more than 30, but there are only 6-12 reference stars in images of 2017 VR12 and 6-10 reference stars were used in images of Midas.

4.3 Midas

In Figures 8 and 9, and Table 8, we compare the $(O-C)$ residuals of Midas by using different ephemerides from JPL and IMCCE. The mean values of $(O-C)$ in right ascension and declination are $-0.023''$ and $-0.047''$ compared with the JPL ephemeris, and $-0.239''$ and $-0.038''$ compared with the IMCCE ephemeris respectively. The dispersions of our observations are estimated to be about $0.081''$ and $0.058''$ in right ascension and declination respectively. Due to the lack of sufficient reference stars, we extend the exposure time to 60 s, but the result becomes worse. Most of the brighter reference stars are distributed in one direction of Midas. In order to obtain enough reference stars to solve the plate constants, sometimes we have to place the target in the corner of the image, which may introduce obvious systematic error due to the geometric distortion of the CCD field of view (Anderson & King 2003; Peng et al. 2012; Peng 2011; Zhang et al. 2012). Therefore, in the next step, the geometric distortion factor should be considered in order to derive more accurate astrometric data.

4.4 Estimation of the Time Recording Error

A CCD camera with good time recording capability is important for obtaining accurate observations, especially for fast moving objects. For the target 2017 VR12, if the timing system has a 1 second systematic error, it will cause at most a $0.7''$ systematic error in the declination direction in this observational campaign. We made some attempts to estimate the error associated with time recording from astrometric observation results. Now we consider the inverse of this problem, e.g., we infer possible time deviation (TD) from the $(O-C)$ results. The possible TD can be obtained from $\mathrm{TD}=\frac{\langle O-C\rangle}{v}$, where v is the motion velocity of the target in right ascension or declination. The results are shown in Figure 10. The points on the left show the results on the first day, and those on the right display the results on the second day. Times from the two days are separated and not related to each other. The error bars are set as $\frac{SD}{v\sqrt{m}}$, where SD is the standard deviation of $\langle O-C\rangle$ and m is the number of observations.

As seen in Figure 10, the TDs have no consistency in right ascension or declination, especially for 2017 VR12 and Midas. The difference could be mainly from the astrometric reduction and accuracy of the ephemeris, rather than the time recording system. As seen in Table 2, the target 2017 VR12 has the fastest motion speed in the declination direction (red circles in Fig. 10), but it has good consistency, and roughly equals 1.2 s.

5 CONCLUSIONS

We have presented the results of our astrometric CCD observations for three asteroids using the 1-m telescope administered by Yunnan Observatories. During the reduction, the *Gaia* DR2 star catalog was used to match the stars in the field of view. We implemented the Astrometrica software tool for astrometric data reduction of CCD images. The ephemerides of INPOP13c from IMCCE and DE431 from JPL show inconsistencies for the asteroid 2017 VR12. We find that the difference between the two ephemerides is about $3''$ in the right ascension direction for the asteroid 2017 VR12. We adopted two centering methods, and found that the centroid method can conspicuously reduce dispersion of the non-Gaussian images compared with the PSF model method. The observations of Camillo and Midas are consistent as based on the two ephemerides, especially for Camillo; the mean $(O - C)$ residuals and standard deviations are under $0.05''$. To derive more accurate astrometric data for NEOs, especially fast moving objects, we should use a precise timing system during observation, and consider the geometric distortion of CCD images in processing the astrometric positions. In addition, some astrometrical effects should be considered carefully.

Acknowledgements We acknowledge support from the staff at the 1-m telescope administered by Yunnan Observatories. This research work is financially supported by the National Natural Science Foundation of China (Grant Nos. 11503083 and 11403101). This work has made use of data from the European Space Agency (ESA) mission *Gaia* (`https://www.cosmos.esa.int/gaia`), processed by the *Gaia* Data Processing and Analysis Consortium (DPAC, `https://www.cosmos.esa.int/web/gaia/dpac/consortium`).
Funding for the DPAC has been provided by national institutions, in particular the institutions participating in the *Gaia* Multilateral Agreement.

References

Anderson, J., & King, I. R. 2003, PASP, 115, 113
Bancelin, D., Colas, F., Thuillot, W., Hestroffer, D., & Assafin, M. 2012, A&A, 544, A15
Gaia Collaboration, Prusti, T., de Bruijne, J. H. J., et al. 2016, A&A, 595, A1
Gaia Collaboration, Brown, A. G. A., Vallenari, A., et al. 2018, A&A, 616, A1
Gronchi, G. F. 2005, Celestial Mechanics and Dynamical Astronomy, 93, 295
Lindegren, L. 1977, A&A, 57, 55
Lindegren, L., Hernández, J., Bombrun, A., et al. 2018, A&A, 616, A2
Nedelcu, D. A., Birlan, M., Souchay, J., et al. 2010, A&A, 509, A27
Peng, Q. 2011, Scientia Sinica Physica, Mechanica & Astronomica, 41, 1126
Peng, Q. Y., Vienne, A., Zhang, Q. F., et al. 2012, AJ, 144, 170
Perna, D., Barucci, M. A., & Fulchignoni, M. 2013, A&A Rev., 21, 65
Qiao, R. C., Cheng, X., Shen, K. X., et al. 2008, MNRAS, 391, 1791
Qiao, R. C., Xi, X. J., Dourneau, G., et al. 2011, MNRAS, 413, 1079
Thuillot, W., Lainey, V., Dehant, V., et al. 2011, in EPSC-DPS Joint Meeting 2011, 1833
Ticha, J., Tichy, M., Kocer, M., & Honkova, M. 2009, Meteoritics and Planetary Science, 44, 1889
Zhang, Q.-F., Peng, Q.-Y., & Zhu, Z. 2012, RAA (Research in Astronomy and Astrophysics), 12, 1451
Zhang, X.-L., Yu, Y., Wang, X.-L., et al. 2015, RAA (Research in Astronomy and Astrophysics), 15, 435